PRAMANA
—journal of
physics

Vol. 50, No. 6,
June 1998
pp. 573–589

Positron scattering by atoms

H R J WALTERS, ANN A KERNOGHAN, MARY T MCALINDEN* and
C P CAMPBELL
Department of Applied Mathematics and Theoretical Physics, The Queen's University of Belfast, Belfast BT7 1NN, United Kingdom
* School of Computing, PO Box 334, Staffordshire University, Beaconside, Stafford ST18 0DG, United Kingdom

Abstract. We describe the present status of coupled-state calculations for positron scattering by 'one-electron' atoms. We show how pseudostates are used to represent the continuum channels. Illustrative results from positron scattering by atomic hydrogen and the alkali metals are presented.

Keywords. Positron; scattering; atom.

PACS No. 34.80

1. Introduction

The past few years have seen considerable advances in the experimental and theoretical study of positron-atom collisions. On the theoretical side these advances have been associated primarily with the development of coupled-state methods for positron collisions with one-electron atoms, i.e., with atomic hydrogen and, in a frozen core approximation, the alkali metals. For these systems there now exist computer programs capable of using large numbers of eigenstates and pseudostates. Here, we shall confine our attention to the achievements of this coupled-state approach. This method has been pioneered by Ghosh and collaborators at the Indian Association for the Cultivation of Science in Calcutta. For a previous, but recent review containing substantially more references, see [1].

In what way does positron-atom scattering differ from electron-atom scattering? Consider positron scattering by ground state atomic hydrogen. The following processes are possible:

$$\begin{aligned} e^+ + \mathrm{H}(1s) &\longrightarrow e^+ + \mathrm{H}(1s) \quad \text{Elastic scattering} \\ &\longrightarrow e^+ + \mathrm{H}(nlm) \quad \text{Atom excitation} \\ &\longrightarrow e^+ + e^- + p \quad \text{Ionization} \\ &\longrightarrow p + \gamma\,\text{rays} \quad \text{Annihilation} \\ &\longrightarrow \mathrm{Ps}(nlm) + p \quad \text{Positronium formation.} \end{aligned} \tag{1}$$

The first three reactions are in common with electron scattering but the last two are particular to the positron. Of these two reactions, positronium formation is the most

important, only at very low impact energies of the positron is annihilation significant. It is the existence of the positronium formation channels that really makes the difference. Positronium formation is a two-centre rearrangement process in which an electron is transferred from a bound orbital centred on the atomic nucleus to a bound orbital around the moving positron. The positronium atom thus created is in essence a very light hydrogen atom of mass [2] 2 au and reduced mass $1/2$ au. In electron-atom scattering one has to deal with the rearrangement process of electron exchange between the incident electron and the target electrons, here, however, the exchange is associated only with a single centre, the atomic nucleus. Theoretically, this one-centre electron exchange is very much easier to treat than the two-centre positronium formation, that is the fundamental technical challenge posed by positron-atom scattering. While we shall not be concerned with the annihilation process here (see (1)), it is worthwhile to remark that it provides a very stringent test of the quality of the calculated collisional wave function. The annihilation cross section depends critically upon the correlation between the positron and the atomic electrons, requiring a knowledge of the values of the collisional wave function when the positron and electron positions coincide. For atoms containing two or more electrons, reactions more exotic than (1) are possible, for example, Ps^- formation, transfer ionization (in which the atom looses two electrons, one to positronium formation, the other electron being directly ionized), multiple ionization, etc. Experimentally, positron-atom collisions are considerably more difficult to study than electron-atom collisions because of the much lower intensity of presently available positron beams (typically 10^{-5} that of an electron beam). Usually the positrons are obtained from a radioactive β^+ decay source such as Na^{22} or Co^{58}. The positrons emerge isotropically from these sources with energies in the region of a few hundred keV and so require considerable moderation, with consequent loss of flux, to obtain a well defined monoenergetic beam of several eV which can be used in an atomic collision experiment. Another problem which complicates the experimental work is the detection of the neutral positronium atom.

2. Coupled-state approximation for positron scattering by atomic hydrogen and the alkali metals

We model the alkali atom in a frozen core approximation. The state of the atom is now synonymous with the state of the valence electron. The interaction of the valence electron with the core is represented by the local central potential

$$\left(-\frac{1}{r_e} - V_e(r_e)\right), \tag{2}$$

where $\mathbf{r}_e$ is the position vector of the electron relative to the nucleus and where we have explicitly removed the long-range ionic tail $-1/r_e$ so that $V_e(r_e)$ is a non-Coulombic potential. Suitable model potentials of the form (2) for Li, Na, K, Rb and Cs may be found in the paper by Stein [3]. In the frozen core approximation (2) the atomic Hamiltonian becomes

$$H_A = -\frac{1}{2}\nabla_e^2 - \frac{1}{r_e} - V_e(r_e). \tag{3}$$

The Hamiltonian, H, describing the positron collision with the frozen core alkali is

$$H = -\frac{1}{2}\nabla_p^2 + H_A + \frac{1}{r_p} + V_p(r_p) - \frac{1}{|\mathbf{r}_p - \mathbf{r}_e|}, \tag{4}$$

where $\mathbf{r}_p$ is the position vector of the positron relative to the nucleus and, in analogy with (2),

$$\left(+\frac{1}{r_p} + V_p(r_p)\right) \tag{5}$$

is the interaction of the positron with the atomic core. The coordinates $(\mathbf{r}_p, \mathbf{r}_e)$ used in writing (4) are those appropriate to positron-atom channels. When positronium is formed it is more appropriate to use the 'positronium coordinates'

$$\mathbf{R} \equiv \frac{\mathbf{r}_p + \mathbf{r}_e}{2}, \quad \mathbf{t} \equiv \mathbf{r}_p - \mathbf{r}_e. \tag{6}$$

Here $\mathbf{R}$ defines the centre of mass of the positronium relative to the nucleus and $\mathbf{t}$ is the positronium internal coordinate. In terms of (6), the Hamiltonian (4) may be equivalently written

$$H = -\frac{1}{4}\nabla_R^2 + H_{Ps} + \left(\frac{1}{|\mathbf{R}+\mathbf{t}/2|} + V_p(|\mathbf{R}+\mathbf{t}/2|)\right) - \left(\frac{1}{|\mathbf{R}-\mathbf{t}/2|} + V_e(|\mathbf{R}-\mathbf{t}/2|)\right). \tag{7}$$

In (7), $-\frac{1}{4}\nabla_R^2$ is the kinetic energy operator for the positronium centre of mass motion, H_{Ps} is the positronium Hamiltonian

$$H_{Ps} = -\nabla_t^2 - \frac{1}{t} \tag{8}$$

and the remaining terms give the interaction of the positronium with the ionic core of the atom. Positron collisions with atomic hydrogen are obtained as a special case of (2) to (8) by setting $V_e = V_p = 0$.

In the coupled-state approximation the collisional wave function Ψ for the system is expanded as

$$\Psi = \sum_a F_a(\mathbf{r}_p)\psi_a(\mathbf{r}_e) + \sum_b G_b(\mathbf{R})\phi_b(\mathbf{t}), \tag{9}$$

where the sum over a is over atom (valence electron) states ψ_a and the sum over b is over positronium states ϕ_b. These states may be either eigenstates or pseudostates. The first sum in (9) represents the atom channels and the second sum represents the positronium channels. It is interesting to note that if the sets of states ψ_a and ϕ_b were complete, then either

$$\sum_a F_a(\mathbf{r}_p)\psi_a(\mathbf{r}_e) \tag{10}$$

or

$$\sum_b G_b(\mathbf{R})\phi_b(\mathbf{t}) \tag{11}$$

alone would give an exact expansion of the system wave function Ψ. In this sense the expansion (9) is over complete, from which it is also clear that the positronium part of the

expansion is not orthogonal to the atom part. In practical terms, however, we do not deal with complete sets of states, we are restricted to finite, and therefore incomplete sets. What matters then is how rapidly the different forms of expansion (9), (10) and (11) converge as the number of states is increased. *A priori*, it is to be expected that a mixed expansion such as (9) will be more quickly convergent as both the atom channels and positronium channels are being directly represented, this is indeed found to be the case. However, some interesting and very informative calculations have been made using the single-centre expansion (10) and a large basis of atom pseudostates [4, 5].

In principle, the expansions (9), (10) and (11) should include both bound and continuum states of the atom/positronium. In practice, it is at this moment not feasible to deal with continuum eigenstates. Instead we introduce pseudostates. These are constructed so that, together with the retained bound eigenstates, they diagonalize the atom/positronium Hamiltonian, i.e.,

$$\begin{aligned} &\langle\psi_a|H_A|\psi_{a'}\rangle = \epsilon_a\delta_{a,a'}, \quad \langle\psi_a|\psi_{a'}\rangle = \delta_{a,a'} \\ &\langle\phi_b|H_{Ps}|\phi_{b'}\rangle = E_b\delta_{b,b'}, \quad \langle\phi_b|\phi_{b'}\rangle = \delta_{b,b'}. \end{aligned} \tag{12}$$

We do not distinguish between true eigenstates and pseudostates in our notation, using ψ_a and ϕ_b for both. A true eigenstate satisfies not only (12) but also

$$H_A\psi_a = \epsilon_a\psi_a, \quad H_{Ps}\phi_b = E_b\phi_b. \tag{13}$$

While pseudostates obey (12), they do not satisfy (13). Figure 1 shows a typical eigenstate energy spectrum for the atom or positronium, consisting of a discrete part, containing an infinite number of states converging to the ionization threshold, followed by a continuous spectrum [6]. The eigenvalues ϵ_a and E_b of (12) will in general be both positive and negative. When an eigenvalue corresponds to a pseudostate we call it the 'pseudostate energy'. Pseudostate energies will be distributed throughout both the discrete and continuous parts of the eigenstate energy spectrum as shown in figure 1. We can think of a pseudostate as being a 'clump' or 'distribution' over eigenstates with the average energy of the 'clump' being the pseudostate energy [7]. Accordingly, we introduce an energy distribution function $f_a(\epsilon)$ for the pseudostate ψ_a by defining

$$f_a(\epsilon) = |\langle\psi_\epsilon|\psi_a\rangle|^2, \tag{14}$$

where by ψ_ϵ we mean an appropriately normalized [8] eigenstate, either bound or continuum, with energy ϵ and with the same angular momentum quantum numbers as the pseudostate ψ_a. Formula (14) is just the probability that ψ_a contains the eigenstate ψ_ϵ. In general the spectrum $f_a(\epsilon)$ will consist of discrete parts, corresponding to the overlap of ψ_a with discrete eigenstates, and a continuous segment. The fraction of the continuum contained in the pseudostate ψ_a is

$$a_a = \int_0^\infty f_a(\epsilon)\mathrm{d}\epsilon = 1 - \sum_m f_a(\epsilon_m), \tag{15}$$

where the sum on m in (15) is over all bound eigenstates with energy ϵ_m. The quality of a pseudostate set may be gauged by how well the pseudostate energies are distributed throughout the eigenstate spectrum, figure 1. As the number of pseudostates is increased the distribution of pseudostate energies can be made denser and so the division of the

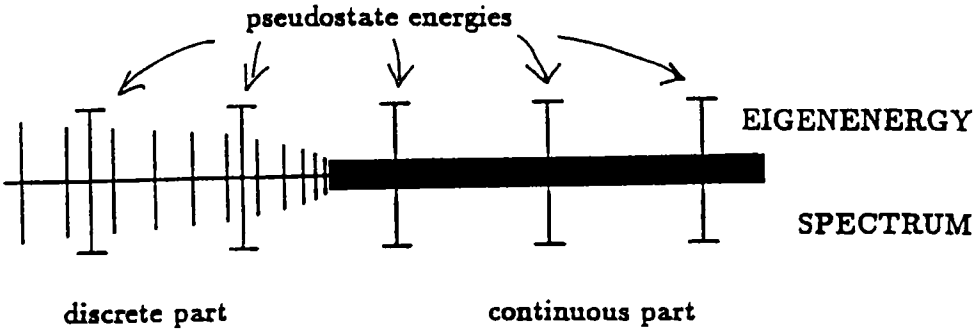

Figure 1.

eigenstates into the 'clumps' which we call pseudostates will become finer, with the result that we approach closer to the ideal of an eigenstate expansion. Surprisingly, in practical terms, this ideal is achieved more quickly than one might suspect, with a manageable number of pseudostates giving a satisfactory representation for most purposes. An inadequate density of pseudostates gives unphysical structures, called pseudostructures, in the calculated cross sections. This was a problem which dogged early pseudostate calculations of electron-atom scattering which did not have the computing power to incorporate enough states. With increasing density of pseudostates these pseudostructures get smaller, until eventually they become negligible.

Pseudostates are usually constructed by diagonalizing the atom/positronium Hamiltonian in a basis of Slater type orbitals

$$r^n e^{-\lambda r/2} Y_{lm}(\hat{\mathbf{r}}), \tag{16}$$

where $\mathbf{r}$ stands for $\mathbf{r}_e$ or $\mathbf{t}$ as appropriate, l is the angular momentum of the state, n is an integer with $n \geq l$, and λ is a parameter which need not be the same for all basis functions (16). It is convenient if the basis can be expanded in a systematic way, for example, by using the same λ for all terms with the same l, taking $n = l, l+1, \ldots, N$, and letting N increase. However, as the powers of r^n go up, this leads to numerical linear dependence problems. This numerical difficulty can be overcome by adopting a Laguerre basis

$$\left(\frac{\lambda^3 (n-l)!}{(n+l+2)!}\right)^{1/2} (\lambda r)^l L_{n-l}^{2l+2}(\lambda r) e^{-\lambda r/2} Y_{lm}(\hat{\mathbf{r}}), \quad n = l, l+1, \ldots, N, \tag{17}$$

where $L_\alpha^\beta(x)$ is a Laguerre polynomial as defined in Gradshteyn and Ryzhik [9]. Mathematically the basis (17) is identical to (16) for the same range of n, i.e., it includes exactly the same powers of r multiplying $e^{-\lambda r/2}$. Numerically, however, it is much more satisfactory in that the functions (17) are mutually orthogonal for different n and the Laguerre polynomials can be generated from a recurrence relation [9] instead of having to be evaluated as a sum of powers of r, which, numerically, would be equivalent to using (16). With the basis (17) there is no problem in diagonalizing the atom/positronium Hamiltonian, for a given l, using 100 or more states [10]. By contrast the basis (16) can fail if the number of states exceeds 15 or so.

Let us now return to the expansion (9). The coupled equations for the functions $F_a(\mathbf{r}_p)$ and $G_b(\mathbf{R})$ are obtained by substituting (9) into the Schrödinger equation with the Hamiltonian (4)/(7), projecting with $\psi_a(\mathbf{r}_e)$ and $\phi_b(\mathbf{t})$, and using (12). The resulting equations are

$$(\nabla_p^2 - 2V_p(r_p) + k_a^2)F_a(\mathbf{r}_p) = 2\sum_{a'} V_{aa'}(\mathbf{r}_p)F_{a'}(\mathbf{r}_p) + 2\sum_{b'}\int K_{ab'}(\mathbf{r}_p,\mathbf{R})G_{b'}(\mathbf{R})\mathrm{d}\mathbf{R}, \tag{18}$$

$$(\nabla_R^2 + p_b^2)G_b(\mathbf{R}) = 4\sum_{b'} U_{bb'}(\mathbf{R})G_{b'}(\mathbf{R}) + 4\sum_{a'}\int K^{\star}_{a'b}(\mathbf{r}_p,\mathbf{R})F_{a'}(\mathbf{r}_p)\mathrm{d}\mathbf{r}_p, \tag{19}$$

where $\star$ stands for complex conjugation and where we assume that the positron is incident with momentum $\mathbf{k}_0$ upon an atomic state of energy ϵ_0 so that

$$\frac{k_a^2}{2} + \epsilon_a = \frac{k_0^2}{2} + \epsilon_0 = \frac{p_b^2}{4} + E_b. \tag{20}$$

The potentials $V_{aa'}(\mathbf{r}_p)$ and $U_{bb'}(\mathbf{R})$ are the direct potentials in the positron-atom and positronium channels respectively and are given by

$$V_{aa'}(\mathbf{r}_p) \equiv \left\langle \psi_a(\mathbf{r}_e)\left|\frac{1}{r_p} - \frac{1}{|\mathbf{r}_e - \mathbf{r}_p|}\right|\psi_{a'}(\mathbf{r}_e)\right\rangle, \tag{21}$$

$$U_{bb'}(\mathbf{R}) \equiv \left\langle \phi_b(\mathbf{t})\left|\left(\frac{1}{|\mathbf{R}+\frac{1}{2}\mathbf{t}|} - \frac{1}{|\mathbf{R}-\frac{1}{2}\mathbf{t}|}\right)\right|\phi_{b'}(\mathbf{t})\right\rangle + \left\langle \phi_b(\mathbf{t})\left|\left(V_p\left(\left|\mathbf{R}+\frac{1}{2}\mathbf{t}\right|\right) - V_e\left(\left|\mathbf{R}-\frac{1}{2}\mathbf{t}\right|\right)\right)\right|\phi_{b'}(\mathbf{t})\right\rangle. \tag{22}$$

However, the most interesting components of (18) and (19) are the non-local couplings $K_{ab}(\mathbf{r}_p,\mathbf{R})$ which have the form [11]

$$K_{ab}(\mathbf{r}_p,\mathbf{R}) = K_{ab}^{(1)}(\mathbf{r}_p,\mathbf{R}) - k_0^2 K_{ab}^{(2)}(\mathbf{r}_p,\mathbf{R}), \tag{23}$$

where

$$K_{ab}^{(1)}(\mathbf{r}_p,\mathbf{R}) \equiv 8\Big\{\left(-\frac{1}{2}\nabla_p^2 + V_p(r_p) - \epsilon_0\right)[\psi_a^{\star}(2\mathbf{R}-\mathbf{r}_p)\phi_b(2\mathbf{r}_p - 2\mathbf{R})] + (H_A\psi_a)^{\star}(2\mathbf{R}-\mathbf{r}_p)\phi_b(2\mathbf{r}_p-2\mathbf{R}) + \psi_a^{\star}(2\mathbf{R}-\mathbf{r}_p)\left(\frac{1}{r_p} - \frac{1}{|2\mathbf{r}_p - 2\mathbf{R}|}\right)\phi_b(2\mathbf{r}_p-2\mathbf{R})\Big\}, \tag{24}$$

$$K_{ab}^{(2)}(\mathbf{r}_p,\mathbf{R}) \equiv 4\psi_a^{\star}(2\mathbf{R}-\mathbf{r}_p)\phi_b(2\mathbf{r}_p-2\mathbf{R}) \tag{25}$$

and the operation ∇_p^2 is to be carried out holding $\mathbf{R}$ fixed. It is the terms (23) which give rise to positronium formation. The coupling $K_{ab}(\mathbf{r}_p,\mathbf{R})$ describes positronium formation in the state ϕ_b by capture of an electron from state ψ_a of the atom, we call $K_{ab}(\mathbf{r}_p,\mathbf{R})$ a positronium formation kernel. It is the evaluation of these kernels and their incorporation

into the coupled equations (18) and (19) which make the theoretical treatment of positron-atom collisions so much more difficult than the sister subject of electron-atom scattering. As stated earlier, the difficulty is the two-centre nature of $K_{ab}(\mathbf{r}_p, \mathbf{R})$ which, in (24) and (25), is apparent in the product $\psi_a^\star(2\mathbf{R} - \mathbf{r}_p)\phi_b(2\mathbf{r}_p - 2\mathbf{R})$. For an atom containing more than one electron equation (19) is even more complicated. To the right hand side of (19) must then be added a term [12]

$$\sum_{b'} \int L_{bb'}(\mathbf{R}, \mathbf{R}')G_{b'}(\mathbf{R}')\mathrm{d}\mathbf{R}'. \tag{26}$$

This term describes electron exchange between positronium in the state $\phi_{b'}$ and the atomic ion, resulting in positronium in the state ϕ_b. The positronium exchange kernels $L_{bb'}(\mathbf{R}, \mathbf{R}')$ are even more complicated to deal with than the positronium formation kernels and only the Calcutta group of Ghosh and co-workers has made substantial progress in incorporating them into calculations, for positron-He scattering [13–15]. The absence of positronium exchange kernels is one advantage of working with one-electron systems.

The coupled-equations (18) and (19) are solved in the partial wave representation where they take the form [11]

$$\left(\frac{\mathrm{d}^2}{\mathrm{d}r_p^2} - \frac{L(L+1)}{r_p^2} - 2V_p(r_p) + k_a^2\right) f^{JL}_{n_a l_a}(r_p) = 2\sum_{n_{a'} l_{a'}} \sum_{L'=|J-l_{a'}|}^{|J+l_{a'}|} V^{JLL'}_{n_a l_a, n_{a'} l_{a'}}(r_p)$$
$$\times f^{JL'}_{n_{a'} l_{a'}}(r_p) + 2\sum_{n_{b'} l_{b'}} \sum_{L'=|J-l_{b'}|}^{|J+l_{b'}|} \int K^{JLL'}_{n_a l_a, n_{b'} l_{b'}}(r_p, R) g^{JL'}_{n_{b'} l_{b'}}(R)\mathrm{d}R, \tag{27}$$

$$\left(\frac{\mathrm{d}^2}{\mathrm{d}R^2} - \frac{L(L+1)}{R^2} + p_b^2\right) g^{JL}_{n_b l_b}(R) = 4\sum_{n_{b'} l_{b'}} \sum_{L'=|J-l_{b'}|}^{|J+l_{b'}|} U^{JLL'}_{n_b l_b, n_{b'} l_{b'}}(R) g^{JL'}_{n_{b'} l_{b'}}(R)$$
$$+ 4\sum_{n_{a'} l_{a'}} \sum_{L'=|J-l_{a'}|}^{|J+l_{a'}|} \int K^{JL'L}_{n_{a'} l_{a'}, n_b l_b}(r_p, R) f^{JL'}_{n_{a'} l_{a'}}(r_p)\mathrm{d}r_p, \tag{28}$$

where

$$V^{JLL'}_{n_a l_a, n_{a'} l_{a'}}(r_p) \equiv \sum_{m_a} \sum_{m_{a'}} C(L, l_a, J; -m_a, m_a, 0) C(L', l_{a'}, J; -m_{a'}, m_{a'}, 0)$$
$$\times \int Y^\star_{L,-m_a}(\hat{\mathbf{r}}_p) V_{aa'}(\mathbf{r}_p) Y_{L',-m_{a'}}(\hat{\mathbf{r}}_p)\mathrm{d}\hat{\mathbf{r}}_p, \tag{29}$$

$$U^{JLL'}_{n_b l_b, n_{b'} l_{b'}}(R) \equiv \sum_{m_b} \sum_{m_{b'}} C(L, l_b, J; -m_b, m_b, 0) C(L', l_{b'}, J; -m_{b'}, m_{b'}, 0)$$
$$\times \int Y^\star_{L,-m_b}(\hat{\mathbf{R}}) U_{bb'}(\mathbf{R}) Y_{L',-m_{b'}}(\hat{\mathbf{R}})\mathrm{d}\hat{\mathbf{R}}, \tag{30}$$

$$K^{JLL'}_{n_a l_a, n_b l_b}(r_p, R) \equiv \sum_{m_a} \sum_{m_b} C(L, l_a, J; -m_a, m_a, 0) C(L', l_b, J; -m_b, m_b, 0)$$
$$\times (Rr_p) \int Y^\star_{L,-m_a}(\hat{\mathbf{r}}_p) K_{ab}(\mathbf{r}_p, \mathbf{R}) Y_{L',-m_b}(\hat{\mathbf{R}})\mathrm{d}\hat{\mathbf{r}}_p\mathrm{d}\hat{\mathbf{R}}. \tag{31}$$

In (27) to (31), J is the total orbital angular momentum of the system (which is conserved),

n_a and l_a (n_b and l_b) are the principal and orbital angular momentum quantum numbers of the state $\psi_a(\mathbf{r})$ ($\phi_b(\mathbf{t})$), ie,

$$\psi_a(\mathbf{r}) = R_{n_a l_a}(r) Y_{l_a m_a}(\hat{\mathbf{r}}), \quad \phi_b(\mathbf{t}) = S_{n_b l_b}(t) Y_{l_b m_b}(\hat{\mathbf{t}}), \tag{32}$$

where Y_{lm} is a spherical harmonic as defined by Rose [16] and unit vectors are denoted by a 'hat', $L(L')$ is the orbital angular momentum of the scattered particle (positron or positronium) about the nucleus, and $C(j_1, j_2, j_3; m_1, m_2, m_3)$ is a Clebsch–Gordan coefficient as given in Rose [16]. A channel is therefore specified by the quantum numbers $JLn_a l_a$ for a positron-atom channel and $JLn_b l_b$ for a positronium-ion channel. In writing (28) we have also used the fact that $K^{JLL'}_{n_a l_a, n_b l_b}(r_p, R)$ is real.

One of the main difficulties in solving the coupled equations (27) and (28) is to render the positronium formation kernels $K^{JLL'}_{n_a l_a, n_b l_b}(r_p, R)$ into a computable form. To illustrate what is involved we consider the procedure used by Walters and co-workers [11]. A typical term from (23) has the structure

$$A(r_p, R, \cos\theta) |2\mathbf{R} - \mathbf{r}_p|^{l_a} Y^{\star}_{l_a m_a}(\widehat{2\mathbf{R} - \mathbf{r}_p}) |2\mathbf{r}_p - 2\mathbf{R}|^{l_b} Y_{l_b m_b}(\widehat{2\mathbf{r}_p - 2\mathbf{R}}), \tag{33}$$

where $\cos\theta$ is the cosine of the angle between $\mathbf{r}_p$ and $\mathbf{R}$. For example, the term

$$\psi^{\star}_a(2\mathbf{R} - \mathbf{r}_p)\left(\frac{1}{r_p} - \frac{1}{|2\mathbf{r}_p - 2\mathbf{R}|}\right)\phi_b(2\mathbf{r}_p - 2\mathbf{R}) \tag{34}$$

in (24) has the structure (33) with

$$A(r_p, R, \cos\theta) \equiv \frac{R_{n_a l_a}(|2\mathbf{R} - \mathbf{r}_p|)}{|2\mathbf{R} - \mathbf{r}_p|^{l_a}} \left(\frac{1}{r_p} - \frac{1}{|2\mathbf{r}_p - 2\mathbf{R}|}\right) \frac{S_{n_b l_b}(|2\mathbf{r}_p - 2\mathbf{R}|)}{|2\mathbf{r}_p - 2\mathbf{R}|^{l_b}}. \tag{35}$$

In calculating (31) we therefore have to evaluate integrals of the form

$$\int Y^{\star}_{L,-m_a}(\hat{\mathbf{r}}_p) |2\mathbf{R} - \mathbf{r}_p|^{l_a} Y^{\star}_{l_a m_a}(\widehat{2\mathbf{R} - \mathbf{r}_p}) A(r_p, R, \cos\theta)$$
$$\times |2\mathbf{r}_p - 2\mathbf{R}|^{l_b} Y_{l_b m_b}(\widehat{2\mathbf{r}_p - 2\mathbf{R}}) Y_{L',-m_b}(\hat{\mathbf{R}}) \mathrm{d}\hat{\mathbf{r}}_p \mathrm{d}\hat{\mathbf{R}}. \tag{36}$$

This can be done analytically if everything can be written in terms of spherical harmonics of $\hat{\mathbf{r}}_p$ and $\hat{\mathbf{R}}$ only. For $A(r_p, R, \cos\theta)$ this is no problem since we can expand as

$$A(r_p, R, \cos\theta) = 2\pi \sum_{\lambda=0}^{\infty} \sum_{\mu=-\lambda}^{+\lambda} A_{\lambda}(r_p, R) Y^{\star}_{\lambda\mu}(\hat{\mathbf{r}}_p) Y_{\lambda\mu}(\hat{\mathbf{R}}), \tag{37}$$

where

$$A_{\lambda}(r_p, R) = \int_0^{\pi} A(r_p, R, \cos\theta) P_{\lambda}(\cos\theta) \sin\theta \mathrm{d}\theta \tag{38}$$

although the projection (38) has to be calculated numerically. For the spherical harmonics in $(\widehat{2\mathbf{R} - \mathbf{r}_p})$ and $(\widehat{2\mathbf{r}_p - 2\mathbf{R}})$ we need the result

$$|\mathbf{r}_1 - \mathbf{r}_2|^l Y_{lm}(\widehat{\mathbf{r}_1 - \mathbf{r}_2}) = \sum_{\lambda=0}^{l} \sum_{\mu=-\lambda}^{+\lambda} (-1)^{\lambda+l} \left[\frac{4\pi(2l+1)!}{(2\lambda+1)!(2l-2\lambda+1)!}\right]^{1/2}$$
$$\times C(\lambda, l-\lambda, l; \mu, m-\mu, m) r_1^{\lambda} r_2^{l-\lambda} Y_{\lambda\mu}(\hat{\mathbf{r}}_1) Y_{(l-\lambda),(m-\mu)}(\hat{\mathbf{r}}_2). \tag{39}$$

A very simple and elegant derivation of this formula has been given by Deb *et al* [17] and Chakrabarti and Dewangan [18]. In addition these latter authors also give some potentially very useful generalizations. Using (33), (37) and (39) a computable expression, containing only a finite number of terms, may be deduced for (31).

Two main options exist for solving the partial wave coupled equations (27) and (28), to solve them in coordinate space, as they presently stand, or to transfer to momentum space and solve for the corresponding partial wave T-matrices. The coordinate space approach has been used by Higgins and Burke [19] and by Walters and co-workers [11] who have both adopted the R-matrix procedure [20], and by Gien and Liu [21] who have employed the Harris–Nesbet algebraic variational method. The R-matrix technique is good at low and intermediate energies where positronium formation is important and is efficient at giving a detailed picture of cross sections over the energy range. In the momentum space formulation coupled integral equations are obtained for the T-matrix elements in which the driving terms are first Born amplitudes. As a result, the first Born approximation is guaranteed and so this approach has advantages at high energies. The momentum space formulation for positron-atom scattering was pioneered by Mandal, Ghosh and Sil [22] and is also the basis of the calculations by Hewitt, Bransden and Noble [23] and by Mitroy and Stelbovics [24].

3. Illustrative examples

3.1 *Positron scattering by atomic hydrogen*

Positron scattering by atomic hydrogen is the simplest possible system and has therefore attracted most attention. In figure 2 we show some samples from the 18-state Ps ($1s$, $2s$, $\overline{3s}$, $\overline{4s}$, $2p$, $\overline{3p}$, $\overline{4p}$, $\overline{3d}$, $\overline{4d}$) + H($1s$, $2s$, $\overline{3s}$, $\overline{4s}$, $2p$, $\overline{3p}$, $\overline{4p}$, $\overline{3d}$, $\overline{4d}$) calculation of Kernoghan *et al* [25] in which $1s$, $2s$ and $2p$ eigenstates and $\overline{3s}$, $\overline{4s}$, $\overline{3p}$, $\overline{4p}$, $\overline{3d}$ and $\overline{4d}$ pseudostates, both of positronium and atomic hydrogen, have been used in the expansion (9). The feature to note here is the 'lumpiness' of the Ps($2p$), H($2s$) and H($2p$) cross sections. These are pseudostructure effects as mentioned in § 2. Also shown in figure 2 is the 33-state Ps($1s$, $2s$, $2p$) + H($1s$, $2s$, $\overline{3s}$ to $\overline{9s}$, $2p$, $\overline{3p}$ to $\overline{9p}$, $\overline{3d}$ to $\overline{9d}$, $\overline{4f}$ to $\overline{9f}$) calculation of Kernoghan *et al* [26]. By contrast, the 33-state cross sections are very much smoother than the 18-state numbers, demonstrating the fact that pseudostructure decreases as the density of pseudostates is increased. It should also be noted that a suitable average through the pseudostructure in the 18-state curves would give an answer close to the 33-state results.

Since pseudostates are primarily designed to represent continuum channels, it is of special interest to see what is predicted for the ionization cross section. Figure 3 shows the 18-state prediction of Kernoghan *et al* [25]. Here the ionization cross section has been calculated from the ansatz

$$\sigma_{\text{ion}} = \sum_i a_i \sigma_{\text{H}}(i) + \sum_j a_j \sigma_{\text{Ps}}(j), \tag{40}$$

where the sum on $i(j)$ runs over the $\overline{3s}$, $\overline{4s}$, $\overline{3p}$, $\overline{4p}$, $\overline{3d}$ and $\overline{4d}$ pseudostates of atomic hydrogen (positronium), $\sigma_{\text{H}}(i)$ ($\sigma_{\text{Ps}}(j)$) is the cross section for exciting the ith (jth) pseudostate of atomic hydrogen (positronium) and a_i (a_j) is the probability (15) that the ith

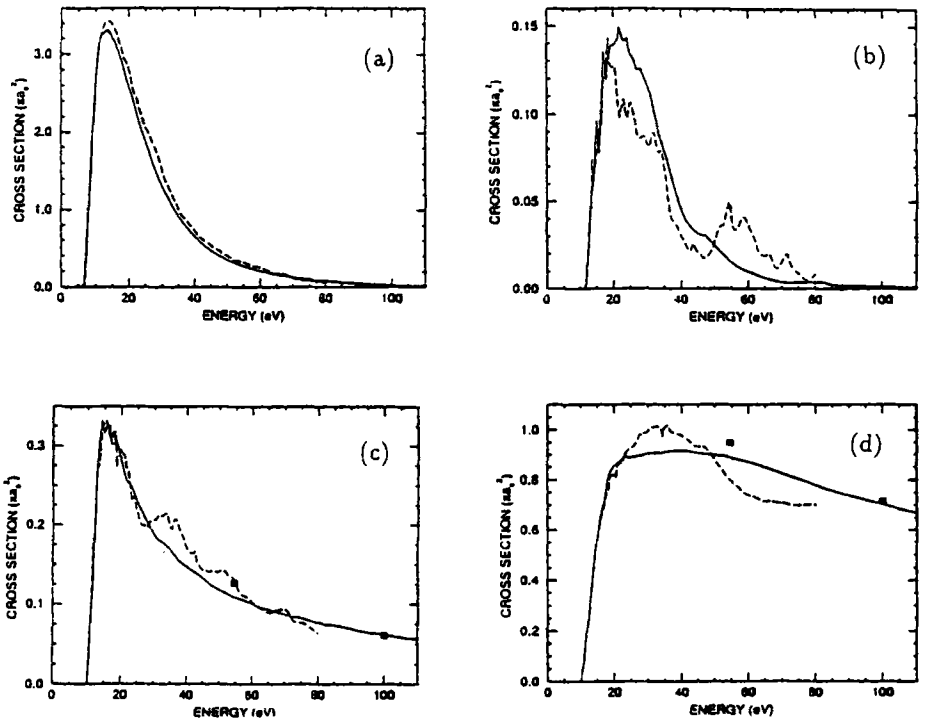

Figure 2. 18-state [25] (dashed curve) and 33-state [26] (solid curve) results for (**a**) Ps(1*s*) formation, (**b**) Ps(2*p*) formation, (**c**) H(2*s*) excitation and (**d**) H(2*p*) excitation. Solid squares are the multipseudostate close-coupling results of Walters [27].

(*j*th) pseudostate overlaps the eigenstate continuum [28]. The computed cross section is in quite good agreement with the measurements of Jones *et al* [29]. Also shown in figure 3 is the contribution to σ_{ion} coming from the atomic hydrogen pseudostates alone, ie, see (40),

$$\sum_i a_i \sigma_{\text{H}}(i). \tag{41}$$

This amounts to little more than 50% of σ_{ion}, demonstrating that, in the energy range shown, the ionization is carried almost equally by the positronium and atomic hydrogen pseudostates. Again, the lumpiness in the curves of figure 3 is pseudostructure.

One obvious difference between the 18-state and 33-state approximations is the use of both positronium and hydrogen pseudostates in the former case, but only hydrogen pseudostates in the latter. Because the atomic hydrogen and positronium components of the system wave function (9) are not orthogonal, it is possible that the ansatz (40) may involve double counting between the positronium and hydrogen contributions. It was to avoid this ambiguity that Kernoghan *et al* [26] decided to use pseudostates only on the atom centre in their 33-state approximation. Then, the ansatz (40) reduces to

$$\sigma_{\text{ion}} = \sum_i a_i \sigma_{\text{H}}(i) \tag{42}$$

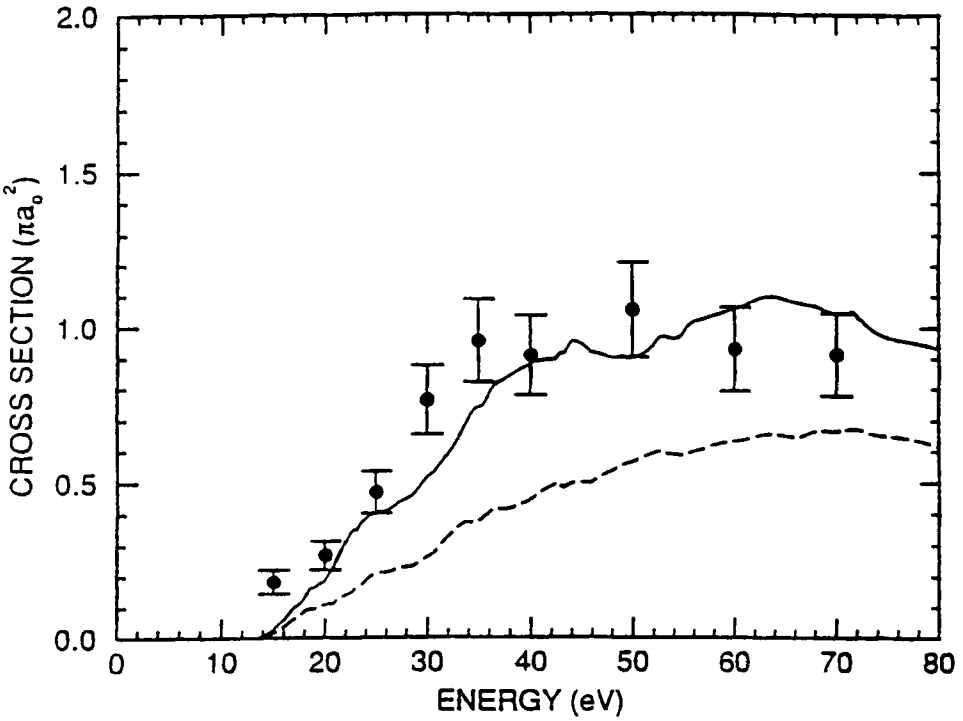

Figure 3. Ionization cross section as calculated in the 18-state approximation of Kernoghan *et al* [25]: solid curve, full cross section (40); dashed curve, contribution (41) from atomic pseudostates alone; solid circles, experimental data of Jones *et al* [29].

and there can be no double counting. Interestingly, the two ionization cross sections, ie, 18-state and 33-state, turn out to be quite comparable, compare figures 3 and 4(b).

Figure 4 shows the agreement that can now be obtained between theory and experiment for positron scattering by atomic hydrogen. Here the 33-state results of Kernoghan *et al* [26] are compared with the positronium formation and total cross section measurements of Zhou *et al* [30] and with the ionization cross sections of Jones *et al* [29]. It is not unreasonable to say that the agreement between theory and experiment is very good.

Figure 5 shows the total cross section and its main components as calculated in the 33-state approximation. This picture underlines the power of the coupled-pseudostate method which gives simultaneously information on all processes. We see from figure 5 that between 8.5 and 35 eV positronium formation is the main contributor to the total cross section, while, above 35 eV ionization and H($2p$) excitation are the largest components and of comparable size. Because of the very good agreement between the 33-state numbers and experiment seen in figure 4, and because of the agreement on average between the 33-state results and those of the 18-state approximation, we believe that the 33-state calculations shown in figure 5 now give the main cross sections for positron scattering off ground state atomic hydrogen to a high degree of accuracy.

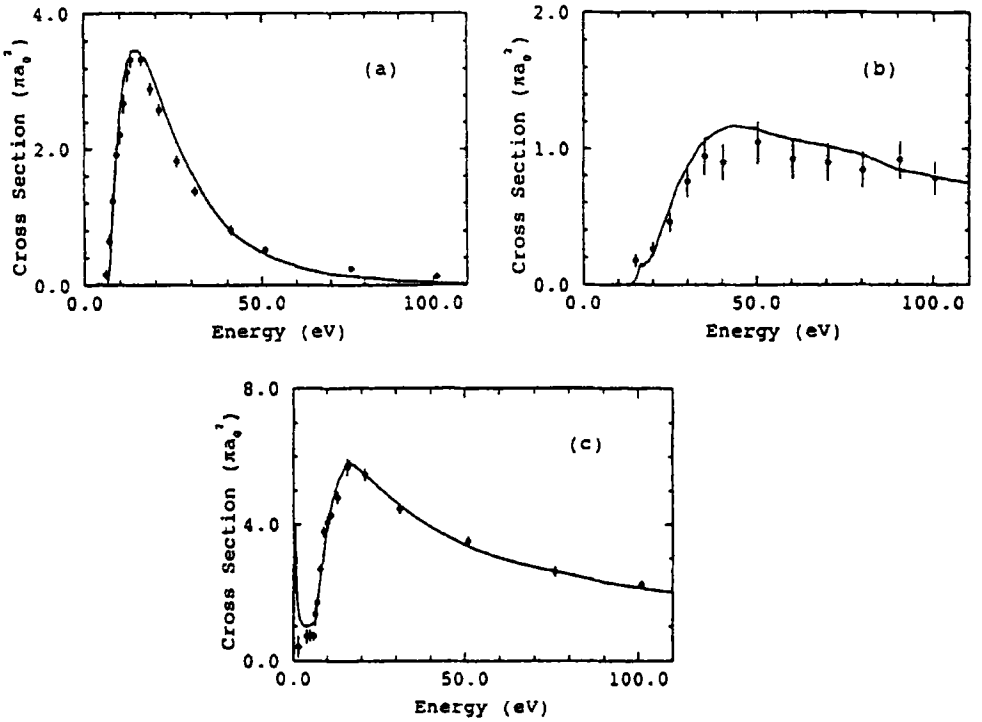

Figure 4. Positron scattering by atomic hydrogen: (**a**) total positronium formation; (**b**) ionization; (**c**) total cross section. Solid curve gives the 33-state results of Kernoghan *et al* [26]. Experimental data are from Jones *et al* [29] and Zhou *et al* [30]. The measurements of Zhou *et al* are shown only with statistical errors, for estimates of other errors see [30].

3.2 *Positron scattering by the alkali metals*

As the ionization potential of an alkali atom is typically around 5 eV, and as the binding energy of Ps($1s$) is 6.8 eV, unlike atomic hydrogen, Ps($1s$) can be formed for all impact energies of the positron on the alkali atom, i.e., the process is exothermic. A consequence of this is that the Ps($1s$) formation cross section becomes infinite as $1/k_0$ at zero impact energy [31].

Figure 6 shows a recent calculation of McAlinden *et al* [32] for positron scattering by Li in a Ps($1s$, $2s$, $2p$) + Li($2s$, $3s$, $\overline{4s}$ to $\overline{9s}$, $2p$, $3p$, $\overline{4p}$ to $\overline{9p}$, $3d$, $\overline{4d}$ to $\overline{9d}$, $\overline{4f}$ to $\overline{9f}$) approximation. This approximation is analogous to the 33-state approximation for atomic hydrogen discussed above. Figure 6 shows that elastic scattering is dominant at low energies [33], this dominance passing directly to the Li($2s$) $\rightarrow$ Li($2p$) excitation with increasing energy; ionization is seen to be almost negligible on the scale of the other cross sections. Comparing figures 5 and 6, we note that the Li cross sections are more than an order of magnitude larger than those for atomic hydrogen, also, unlike atomic hydrogen, the total positronium formation cross section is never dominant [33].

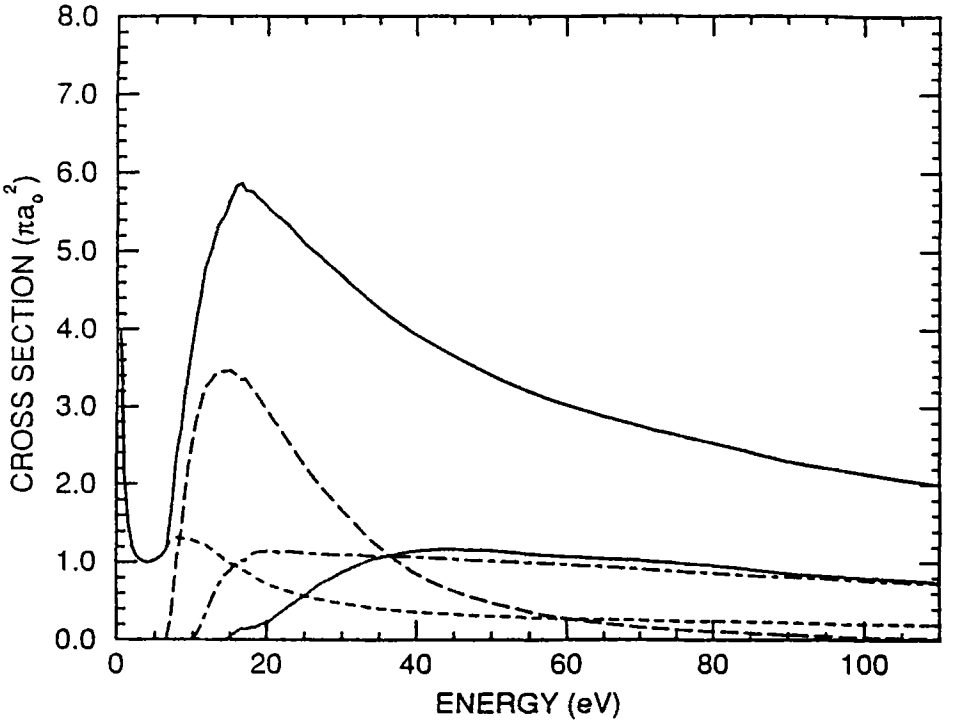

Figure 5. Cross sections in the 33-state approximation [26]: upper solid curve, total cross section; long-dashed curve, total positronium formation; short-dashed curve, elastic scattering; dash-dot curve, H(2*p*) excitation; lower solid curve, ionization.

Coupled-eigenstate calculations have shown a very interesting behaviour as we ascend the alkali metal sequence from Li to Cs. This is illustrated in figures 7 and 8 which show results for positronium formation and total scattering calculated in the approximations [11, 31, 32, 34, 35]:

(i) Ps(1*s*, 2*s*, 2*p*) + Li(2*s*, 2*p*, 3*s*, 3*p*, 3*d*)
(ii) Ps(1*s*, 2*s*, 2*p*) + Na(3*s*, 3*p*, 3*d*, 4*s*, 4*p*)
(iii) Ps(1*s*, 2*s*, 2*p*, 3*s*, 3*p*, 3*d*) + K(4*s*, 4*p*, 5*s*, 5*p*, 3*d*)
(iv) Ps(1*s*, 2*s*, 2*p*, 3*s*, 3*p*, 3*d*) + Rb(5*s*, 5*p*, 6*s*, 6*p*, 4*d*)
(v) Ps(1*s*, 2*s*, 2*p*, 3*s*, 3*p*, 3*d*) + Cs(6*s*, 6*p*, 7*s*, 7*p*, 5*d*).

Figure 7(a) reveals a dramatic collapse in the ground state Ps(1*s*) formation cross section on ascending the series from Li to Cs, while figure 7(b) shows a corresponding inflation in the cross section for positronium formation in excited states. The overall effect is to give a total positronium formation cross section which is peaked at an energy of about 1 eV for Li and Na, but which displays a broad maximum near 6 eV for K, Rb and Cs, this is illustrated for Li and Cs in figure 7(c). Figure 8 also indicates a similar division between the total cross sections for Li and Na, on the one hand, and those for K, Rb and Cs on the other. The Li and Na total cross sections are peaked near 1 eV while the K, Rb and Cs cross sections, again, peak near 6 eV. The broad maximum in these last

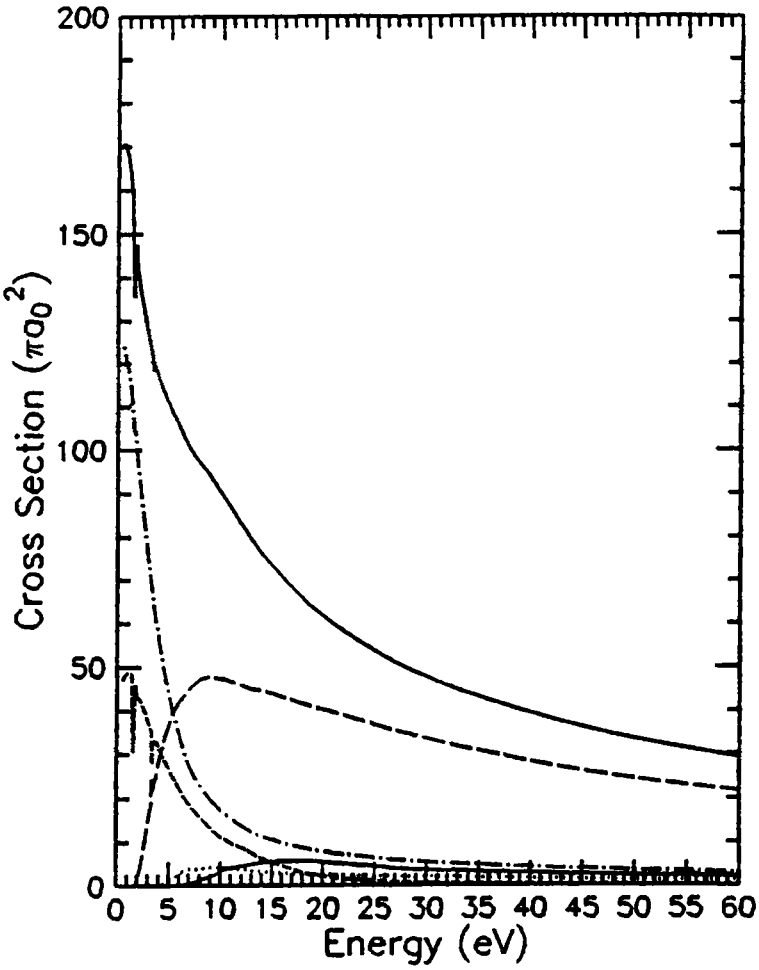

Figure 6. Cross sections for positron scattering by Li in a Ps(1s, 2s, 2p) + Li(2s, 3s, $\overline{4s}$ to $\overline{9s}$, 2p, 3p, $\overline{4p}$ to $\overline{9p}$, 3d, $\overline{4d}$ to $\overline{9d}$, $\overline{4f}$ to $\overline{9f}$) approximation [32]: upper solid curve, total cross section; dash-dot curve, elastic scattering; long-dashed curve, Li(2s) → Li(2p) excitation; short-dashed curve, total positronium formation; dotted curve, Li (2s) → Li (n = 3); lower solid curve, ionization.

three cases derives primarily, although not entirely, from the peak in the excited state positronium formation cross sections of figure 7(b).

Measurements of total positronium formation and total scattering have been made for Na, K and Rb targets by the Detroit group [36–40]. Generally the agreement between theory and experiment is good [11, 31, 32, 34, 35].

4. Conclusion

Coupled-state methods have proved to be a very powerful tool for studying positron-atom scattering. When pseudostates are included in the expansion to represent ionization

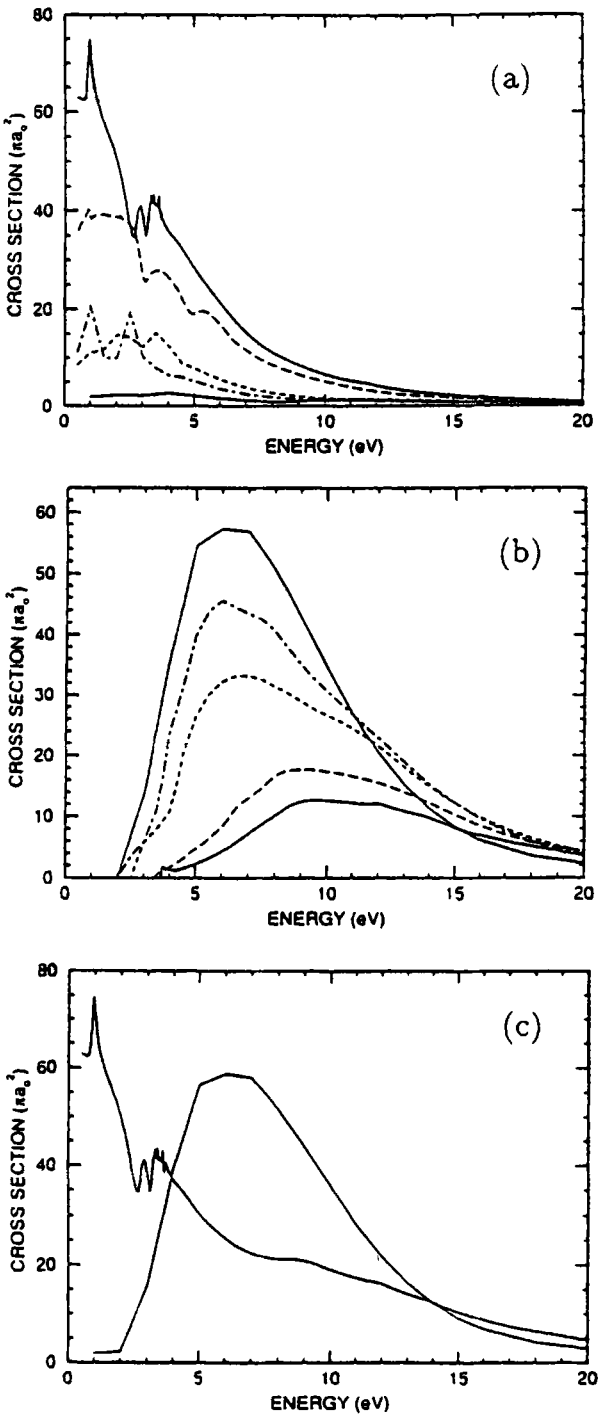

Figure 7. Positronium formation cross sections for Li, Na, K, Rb and Cs: (**a**) Ps(1*s*) formation; (**b**) positronium formation in excited states; (**c**) total positronium formation. Curves: solid, Li; long-dashed, Na; short-dashed, K; dash-dot, Rb; dotted, Cs.

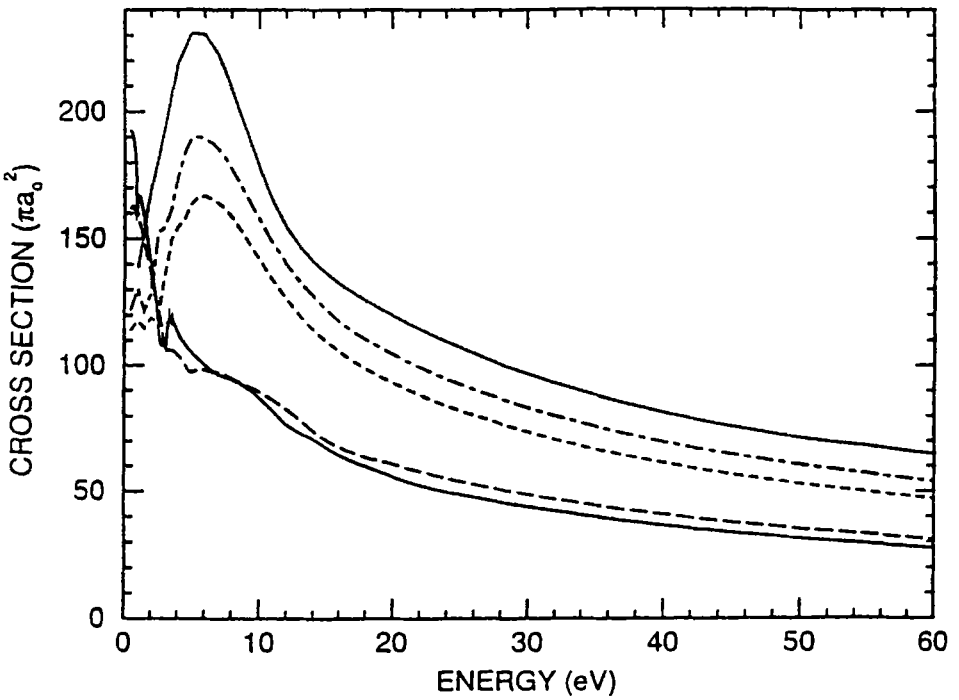

Figure 8. Total cross sections for positron scattering by Li, Na, K, Rb and Cs. Curves: lower solid, Li; long-dashed, Na; short-dashed, K; dash-dot, Rb; upper solid, Cs.

channels, we have, in effect, a complete dynamical theory. The success of this approach is well illustrated by the calculations of positron scattering by ground state atomic hydrogen where we have seen a remarkable convergence between theory and experiment, figure 4. For this system, we believe that we now know the main cross sections to a high degree of accuracy. Where ionization is not so important, as with the alkali metals, coupled-eigenstate approximations seem to give roughly correct results [32]. An important prediction to come out of these calculations is the pronounced growth in excited positronium formation as the alkali metal series is ascended from Li to Cs. This prediction awaits experimental confirmation.

Acknowledgements

The authors are indebted to G Laricchia for advice on experimental aspects of positron-atom collisions.

References

[1] H R J Walters, A A Kernoghan and M T McAlinden, in *The Physics of Electronic and Atomic Collisions (invited papers of the XIX ICPEAC)* edited by L J Dubë, J B A Mitchell, J W McConkey and C E Brion, AIP Conf. Proc. **360**, 397 (1995)

[2] Throughout this article we use atomic units (au) in which $\hbar = m_e = e = 1$. The symbol a_0 is used to denote the Bohr radius
[3] M Stein, *J. Phys.* **B26**, 2087 (1993)
[4] K Higgins, P G Burke and H R J Walters, *J. Phys.* **B23**, 1345 (1990)
[5] I Bray and A T Stelbovics, *Phys. Rev.* **A49**, R2224 (1994)
[6] Consistent with (3) and (8), the ionization threshold is taken to be at zero energy, bound eigenstates have negative energies, continuum eigenstates positive energies
[7] H R J Walters, in *Electronic and Atomic Collisions (invited papers of the XV ICPEAC)* edited by H B Gilbody, W R Newell, F H Smith and A C H Smith (North-Holland, Amsterdam, 1988) p. 147
[8] (14) assumes that bound eigenstates ψ_ϵ are normalised to unity and continuum eigenstates to $\langle\psi_\epsilon|\psi_{\epsilon'}\rangle = \delta(\epsilon - \epsilon')$
[9] I S Gradshteyn and I M Rhyzhik, *Table of Integrals, Series and Products* (Academic Press, New York, 1980)
[10] I Bray, D A Konovalov and I E McCarthy, *Phys. Rev.* **A43**, 1301 (1991)
[11] A A Kernoghan, PhD Thesis, *Positron Scattering by Atomic Hydrogen and the Alkali Metals* (The Queen's University of Belfast, 1996)
[12] In writing (26) we have assumed that electron capture from the atom results in a unique ion state. More generally, G_b, $L_{bb'}$ and K_{ab} would have to carry indices i and i' as well as b and b' to indicate the state of the ion
[13] M Kahali, S K Adhikari, D Basu and A S Ghosh, *Chem. Phys. Lett.* **239**, 344 (1995)
[14] S K Adhikari and A S Ghosh, *Chem. Phys. Lett.* **262**, 460 (1996)
[15] P Chaudhuri, S K Adhikari and A S Ghosh, *J. Phys.* **B30**, L81 (1997)
[16] M E Rose, *Elementary Theory of Angular Momentum* (Wiley, New York, 1957)
[17] N C Deb, N C Sil and P Mandal, *Indian J. Phys.* **B68**, 267 (1994)
[18] S Chakrabarti and D P Dewangan, *J. Phys.* **B28**, L769 (1995)
[19] K Higgins and P G Burke, *J. Phys.* **B24**, 4269 (1993)
[20] P G Burke and W D Robb, *Adv. At. Mol. Phys.* **11**, 143 (1975)
[21] G Liu and T T Gien, *Phys. Rev.* **A46**, 3918 (1992)
[22] P Mandal, A S Ghosh and N C Sil, *J. Phys.* **B8**, 2377 (1975)
[23] R N Hewitt, C J Noble and B H Bransden, *J. Phys.* **B23**, 4185 (1990)
[24] J Mitroy and A T Stelbovics, *Phys. Rev. Lett.* **72**, 3495 (1994)
[25] A A Kernoghan, M T McAlinden and H R J Walters, *J. Phys.* **B28**, 1079 (1995)
[26] A A Kernoghan, D J R Robinson, M T McAlinden and H R J Walters, *J. Phys.* **B29**, 2089 (1996)
[27] H R J Walters, *J. Phys.* **B21**, 1893 (1988)
[28] For the states used by Kernoghan *et al* [25] in their 18-state approximation, a_i has the same value for corresponding hydrogen and positronium pseudostates
[29] G O Jones, M Charlton, J Slevin, G Laricchia, Á. Kövér, M R Poulsen and S Nic Chormaic, *J. Phys.* **B26**, L483 (1993)
[30] S Zhou, H Li, W E Kauppila, C K Kwan and T S Stein, *Phys. Rev.* **A55**, 361 (1997)
[31] M T McAlinden, A A Kernoghan and H R J Walters, *Hyperfine Interactions* **89**, 161 (1994)
[32] M T McAlinden, A A Kernoghan and H R J Walters, *J. Phys.* **B30**, 1543 (1997)
[33] Except, of course, at very low energies where the Ps(1*s*) formation cross section becomes infinite as $1/k_0$
[34] M T McAlinden, A A Kernoghan and H R J Walters, *J. Phys.* **B29**, 555 (1996)
[35] A A Kernoghan, M T McAlinden and H R J Walters, *J. Phys.* **B29**, 3971 (1996)
[36] C K Kwan, W E Kauppila, R A Lukaszew, S P Parikh, T S Stein, Y J Wan and M S Dababneh, *Phys. Rev.* **A44**, 1620 (1991)
[37] S P Parikh, W E Kauppila, C K Kwan, R A Lukaszew, D Przybyla, T S Stein and S Zhou, *Phys. Rev.* **A47**, 1535 (1993)
[38] W E Kauppila, C K Kwan, T S Stein and S Zhou, *J. Phys.* **B27**, L551 (1994)
[39] S Zhou, S P Parikh, W E Kauppila, C K Kwan, D Lin, A Surdutovich and T S Stein, *Phys. Rev. Lett.* **73**, 236 (1994)
[40] A Surdutovich, J Jiang, W E Kauppila, C K Kwan, T S Stein and S Zhou, *Phys. Rev.* **A53**, 2861 (1996)